

# ChemComm

Chemical Communications

Accepted Manuscript

This article can be cited before page numbers have been issued, to do this please use: T. Aizawa, K. Aratsu, S. Datta, T. Mashimo, T. Seki, T. Kajitani, F. Silly and S. Yagai, *Chem. Commun.*, 2020, DOI: 10.1039/D0CC01636E.



This is an Accepted Manuscript, which has been through the Royal Society of Chemistry peer review process and has been accepted for publication.

Accepted Manuscripts are published online shortly after acceptance, before technical editing, formatting and proof reading. Using this free service, authors can make their results available to the community, in citable form, before we publish the edited article. We will replace this Accepted Manuscript with the edited and formatted Advance Article as soon as it is available.

You can find more information about Accepted Manuscripts in the [Information for Authors](#).

Please note that technical editing may introduce minor changes to the text and/or graphics, which may alter content. The journal's standard [Terms & Conditions](#) and the [Ethical guidelines](#) still apply. In no event shall the Royal Society of Chemistry be held responsible for any errors or omissions in this Accepted Manuscript or any consequences arising from the use of any information it contains.

## COMMUNICATION

Received 00th January  
20xx,**Hydrogen bond-directed supramolecular polymorphism leading to soft and hard molecular ordering**Takumi Aizawa,<sup>a</sup> Keisuke Aratsu,<sup>a</sup> Sougata Datta,<sup>b</sup> Takaki Mashimo,<sup>c</sup> Tomohiro Seki,<sup>c</sup>  
Takashi Kajitani,<sup>d</sup> Fabien Silly<sup>e</sup> and Shiki Yagai<sup>\*b,f</sup>

Accepted 00th January 20xx

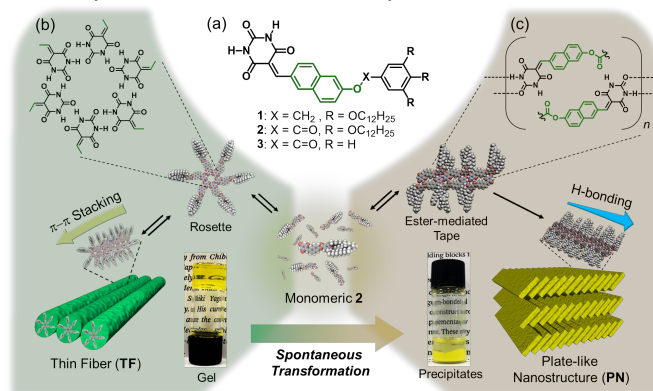
DOI: 10.1039/x0xx00000x

**Transformation of metastable supramolecular stacks of hydrogen-bonded rosettes composed of an ester-containing barbiturated naphthalene into crystalline nanosheet occurs through the rearrangement of hydrogen-bonding patterns. The involvement of the ester group in the crystalline hydrogen-bonded pattern is demonstrated, guiding us to a new molecular design that can afford supramolecular polymorphs with soft and hard molecular packing.**

A phenomenon wherein a molecule has various stable and metastable assembled states can be called supramolecular polymorphism, and is recently increasing attention in the field of supramolecularly engineered soft materials.<sup>1</sup> The phenomenon is caused by an interplay of different self-assembly pathways, bringing in time-evolving dynamic nature. Because the properties of supramolecular materials are highly dependent on the molecular packing structure,<sup>2</sup> designing supramolecular polymorphism beforehand is crucially significant. In particular, it has been rarely reported for single supramolecular building blocks that can form polymorphs whose softness/hardness are dramatically different.<sup>3</sup>

A pragmatic approach is to use building blocks that can produce distinctly different hydrogen-bonded architectures through directional multiple hydrogen bonds.<sup>4</sup> Griesser and co-workers<sup>5</sup> reported that barbituric acid is one of the multiple

hydrogen bonding unit that gives rise to specific polymorphisms derived from a variety of hydrogen bonding patterns depending on the external environment. Most reported structures are based on open-ended tapelike hydrogen-bonded motifs. In contrast, in recent years we have developed unique supramolecular systems organized from cyclic hydrogen-bonded hexamer of barbituric-acid-functionalized (barbiturated)  $\pi$ -conjugated molecules such as **1** bearing wedge-shaped aliphatic tails.<sup>6</sup> These cyclic hexamers, referred to as “rosettes”,<sup>7</sup> stack through  $\pi$ - $\pi$  interactions to afford supramolecular polymers with an intrinsic curvature. Extending this hierarchical process has also led to supramolecular polymers with diverse topologies such as rods,<sup>8</sup> toroids (by **1**),<sup>8a,9</sup> and helicoids,<sup>10</sup> and even chimeric topologies.<sup>11</sup> Almost all the barbiturated  $\pi$ -conjugated molecules with an aliphatic wedge<sup>12</sup> have provided rosette-based supramolecular polymers, but very recently we encountered an exceptional molecule that provides crystalline ribbons which are totally different from rosette-based supramolecular polymers in terms of morphology as well as chemical properties.<sup>13</sup> Although we could not define the underpinning hydrogen-bonded patterns, it was obvious that the presence of an ester linkage in the molecular structure is the key to form such a dramatically different structure.



<sup>a</sup> Division of Advanced Science and Engineering, Graduate School of Science and Engineering, Chiba University, 1-33 Yayoi-cho, Inage-ku, Chiba 263-85223, Japan.

<sup>b</sup> Department of Applied Chemistry and Biotechnology, Graduate School of Engineering, Chiba University, 1-33 Yayoi-cho, Inage-ku, Chiba 263-8522, Japan.

<sup>c</sup> Division of Applied Chemistry and Frontier Chemistry Center (FCC) Faculty of Engineering, Hokkaido University Kita 13 Nishi 8 Kita-ku, Sapporo, Hokkaido 060-8628, Japan.

<sup>d</sup> Suzukakedai Materials Analysis Division, Technical Department, Tokyo Institute of Technology, 4259 Nagatsuta, Midori-ku, Yokohama 226-8503, Japan.

<sup>e</sup> Université Paris-Saclay, CEA, CNRS, SPEC, TITANS, F-91191 Gif sur Yvette, France.

<sup>f</sup> Institute for Global Prominent Research (IGPR), Chiba University, 1-33 Yayoi-cho, Inage-ku, Chiba 263-8522, Japan.

† Footnotes relating to the title and/or authors should appear here.

Electronic Supplementary Information (ESI) available: [details of any supplementary information available should be included here]. See DOI: 10.1039/x0xx00000x

**Fig. 1** (a) Molecular structures of compounds **1**, **2** and **3**. (b,c) Schematic representation of supramolecular polymorph of **2**. Photographs in (b) and (c) show gel of **TF** and precipitates of **PN** formed by **2** ( $c = 1.0 \times 10^{-2}$  M).

Toward a new direction of the self-assembly of barbiturated  $\pi$ -conjugated molecules, herein we investigated self-assembly of simple naphthalene molecule **2** involving an ester linkage. We reveal that molecule **2** kinetically organizes into supramolecular polymers, which in turn transforms into thermodynamically stable crystalline assembly through the rearrangement of hydrogen-bonding pattern (Fig. 1). Remarkably, we successfully revealed the single crystal structure of a reference compound **3** lacking wedge unit, which provides clear evidence that the ester unit is involved in the formation of thermodynamically attained hydrogen-bonded polymeric arrays.

According to our accumulated protocol that organizes barbiturated molecules through the formation of rosettes, we initially examined self-assembly of **2** ( $c = 1.0 \times 10^{-4}$  M) in methylcyclohexane (MCH) by cooling a molecularly-dissolved solution from 80 °C to 20 °C at a rate of 1 °C min<sup>-1</sup>. At 80 °C, **2** showed a vibronic absorption band with a maximum at 362 nm (Fig. 2a). Upon cooling, this absorption band hypsochromically shifted to 350 nm with the emergence of a new absorption in 420–480 nm. This spectral change by cooling proceeded non-sigmoidally as a function of temperature descent, which is characteristic of cooperative supramolecular polymerization mechanism (inset in Fig. 2a).<sup>14</sup> Because the subsequent heating of the as-cooled solution did not show thermal hysteresis, we analysed the cooling curves obtained at several concentrations with a nucleation-elongation model (Fig. S2).<sup>14b</sup> A van't Hoff analysis of the collected data provided an elongation enthalpy  $\Delta H^\circ$  of  $-58$  kJ mol<sup>-1</sup>, which is smaller than that of **1** ( $\Delta H^\circ = -72$  kJ mol<sup>-1</sup>). At 20 °C, the solution showed a green emission with the emission maxima at 530 nm (fluorescence quantum yield:  $\Phi_f = 0.022$ ) (Fig. 2b). When the solution was spin-coated onto highly oriented pyrolytic graphite (HOPG) substrate, atomic force microscopy (AFM) image showed bundled thin fibers (**TF**) with the width and thickness of  $5.98 \pm 1.01$  nm and  $2.32 \pm 0.49$  nm, respectively (Fig. 2c). The width is in good accordance with the diameter of rosette model of **2** (ca. 7 nm) (Fig. 2d and Fig. S1a, S3). The observed morphology is quite different from well-defined toroidal morphology of **1** with highly uniform curvature.<sup>9a,10c</sup> Density functional theory (DFT) calculation revealed that the trialkoxyphenyl wedge unit of **2** has a larger dipole moment compared to that of **1** due to the electron-withdrawing ester group (Fig. S4). We thus inferred that the dipole-dipole interaction between wedge units competes the  $\pi$ - $\pi$  stacking interaction of the rosettes of **2**, which prevents uniform rotational and translational displacements that are prerequisite to form intrinsic curvature.<sup>15</sup>

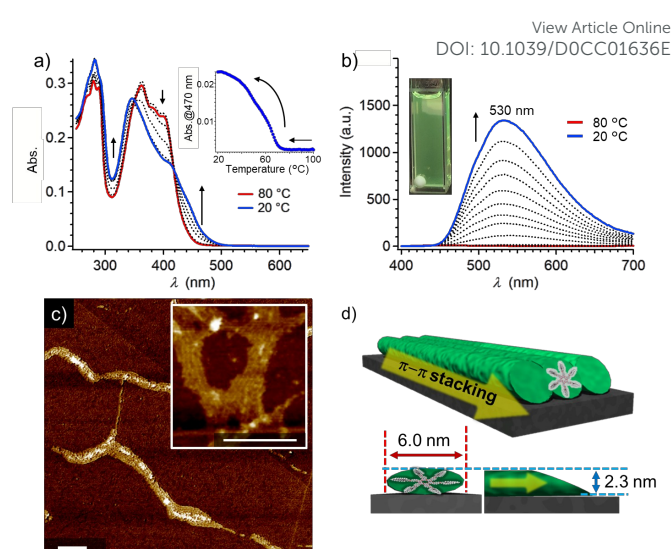


**Fig. 2** (a,b) Temperature-dependent changes of (a) UV-Vis and (b) fluorescence spectra ( $\lambda_{\text{ex}} = 346$  nm) of **2** in MCH ( $c = 1.0 \times 10^{-4}$  M) upon cooling from 80 to 20 °C at a rate of 1 °C min<sup>-1</sup>. Inset in (a) shows a plot of absorbance at 470 nm versus temperature. Inset in (b) is a photograph of the cooled solution under 365-nm light illumination. (c) AFM image of **TF** spin-coated immediately after cooling a MCH solution of **2** ( $c = 1.0 \times 10^{-4}$  M) from 80 to 20 °C at a cooling rate of 1 °C min<sup>-1</sup>. Inset in (c) is another AFM image of **TF** ( $c = 2.5 \times 10^{-4}$  M). Scale bar = 100 nm. (d) Schematic representation of **TF** formed by rosettes.

Despite the fragility of **TF** in the diluted condition, a kinetic supramolecular polymerization of **2** in MCH by quenching hot solutions resulted in gelation at concentrations above  $2.0 \times 10^{-3}$  M (Fig. 1b). Since this observation implies the formation of well-defined one-dimensional aggregates, we assessed the packing structure of **2** in the bulk state. Differential scanning calorimetry (DSC) and polarized optical microscopy revealed that **2** forms a thermotropic liquid crystalline mesophase in the temperature range of 109–194 °C upon cooling from isotropic state (Fig. S5a,b). The X-ray diffraction (XRD) measurement of the mesophase revealed the formation of a hexagonal columnar structure (Col<sub>h</sub>) with lattice constant  $a$  of 5.71 nm (Fig. S5c). This lattice constant is in good agreement with the width of **TF** estimated by AFM. We further found a periodicity of 0.34 nm, which could be attributed to the center-to-center distance of stacked disks (intracolumnar periodicity, or lattice constant  $c$ ) (Fig. S5c). Assuming the density of **2** to be 1.0 g cm<sup>-3</sup>,<sup>8a</sup> the number of molecule per columnar slice of 0.34 nm is calculated to be 6.2, which strongly supports the formation of hexameric rosettes (Fig. S5d,e).<sup>8a</sup> Accordingly, the rosettes of **2** can be densely packed into the hexagonal columnar structure in the condensed phases, whereas in the diluted solution such columnar structures cannot maintain their shapes as shown by the ambiguous AFM image of **TF**, probably due to competition between the wedge units and naphthalene unit.

Reflecting the weakened interaction between rosettes, **TF** is stable only kinetically. At  $c = 5.0 \times 10^{-4}$  M, the **TF** solution remained homogeneous for 10 h at room temperature, thereafter it completely precipitated within 12 h. Similarly, the gel solution shown in Fig. 1b resulted in precipitation within a

day (Fig. 1c). AFM images of the precipitates visualized layered platelike nanostructures (**PN**) with constant thickness of about  $3.64 \pm 0.39$  nm (Fig. 3a). Precipitated **PN** exhibited more yellowish emission at 570 nm ( $\Phi_f = 0.097$ ) compared with **TF** (Fig. 3b). Powder XRD analysis of **PN** displayed a number of peaks (Fig. 3c and S6), suggesting the crystalline nature of this nanostructure. The diffractions in the small-angle region could be assigned as two sets of lamellar structures with periodicities of 3.74 and 1.33 nm (yellow and pink diffractions in Fig. 3c, respectively). The former value showed good agreement with the thickness of **PN** obtained by the AFM images, and the latter is considered to be the in-plane diffraction (vide infra). In the Fourier transform infrared (FT-IR) spectra, some C=O stretching bands of **PN** were observed at frequencies considerably different from those of **TF** (Fig. 3d). Among three bands *a*, *c* and *d* that can be assigned to each of the three C=O groups of the barbituric acid unit, the bands *a* and *d* displayed low and high frequency shifts, respectively. These shifts suggest that **TF** and **PN** are based on different hydrogen bonding patterns. Furthermore, the C=O stretching band *b* derived from the ester group displayed a low frequency shift in **PN** (Fig. 3d), suggesting its involvement in the supramolecular interactions to form **PN**.

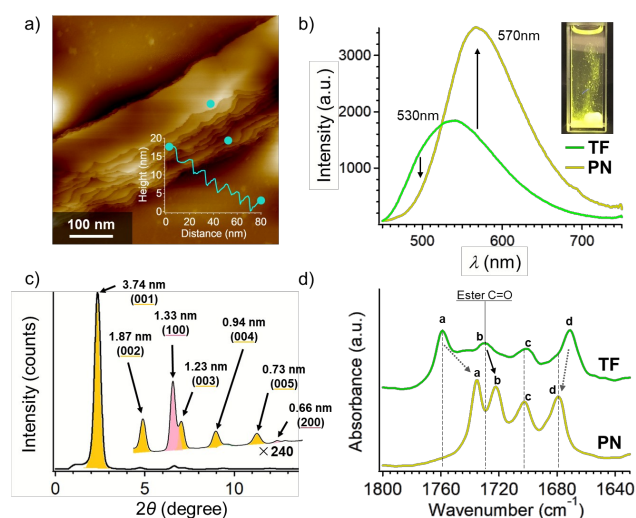


**Fig. 3** (a) AFM image of **PN**. Inset shows cross-sectional analysis of **PN** between the blue dots. (b) Fluorescence spectra of **TF** solution and **PN** suspension in MCH ( $c = 1.0 \times 10^{-4}$  M). Inset in (b) is a photograph of precipitated **PN** under 365 nm-light illumination. (c) Powder XRD pattern of **PN**. (d) FT-IR spectra of **TF** solution and **PN** suspension in MCH ( $c = 5.0 \times 10^{-4}$  M).

To obtain more detailed insight into the supramolecular packing structure of **PN**, we performed X-ray crystallographic analysis for a single crystal of an analogous molecule **3** which lacks the aliphatic tails (Fig. 4a and S7, Table S1). The single crystals of **3** were obtained by diffusing toluene (poor solvent) vapor to a THF (good solvent) solution. The single-crystal structure revealed the formation of an antiparallel dimeric unit of **3** held together by double hydrogen bonds between a NH group of barbituric acid unit and the ester C=O group (green

dotted lines in Fig. 4a). The dimer units are then further connected through double hydrogen bonds between barbituric acid units (orange dotted lines in Fig. 4a). In this structure, the periodicity along to the hydrogen-bonded array of **3** was estimated to be 1.27 nm (Fig. 4a). This periodicity might correspond to the in-plane periodicity of **PN** at  $d = 1.33$  nm (Fig. 3c).

To further correlate the crystal structure of **3** and the supramolecular packing structure of **2**, we investigated a two-dimensional organization of **2** at the liquid–solid interface by using scanning tunnelling microscopy (STM). STM imaging showed the formation of two types of lamellar domains, one major and the other minor domains, with different lamellar molecular arrays (Fig. 4b and S8). In the major domain (domain I), hydrogen bond formation seems to be neglected to form a dense molecular packing (Fig. S8a,b). In the minor domain (domain II), a tilted molecular arrangement could be seen (Fig. 4c and S8c,d), which can be fitted with the ester-mediated hydrogen-bonded supramolecular array found in the crystal structure of **3**. This finding demonstrates that molecule **2** can also organize through a similar ester-mediated hydrogen-bonding motif. In the homogeneous solution phase, the resulting hydrogen-bonded chains presumably assemble into two-dimensional direction with face-to-face slipped  $\pi$ -stacking motif to form **PN** (Fig. 4d), which is also supported by the two-dimensional organization of **3** in the crystal (Fig. S7).

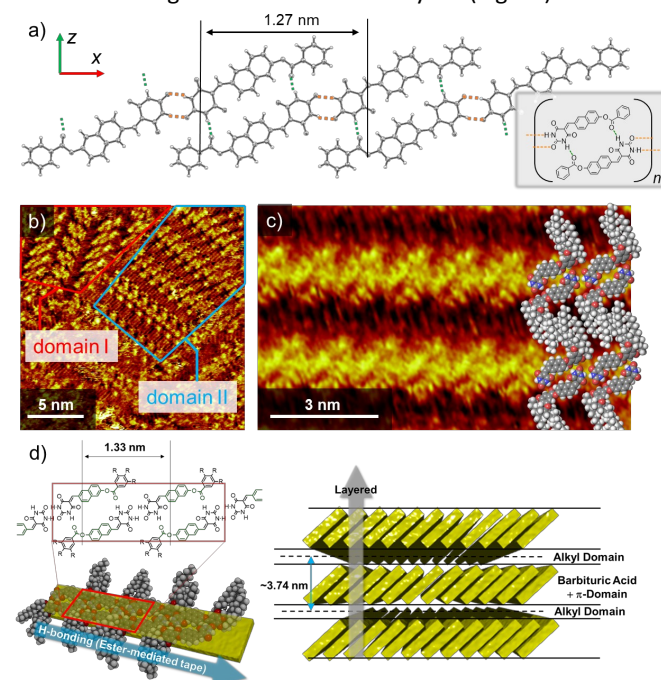


**Fig. 4** (a) Single-crystal structure of **3** along *x* axis (hydrogen-bonding direction). Green dotted lines show hydrogen bonds between a NH of barbituric acid and the C=O of ester group. Orange dotted lines show hydrogen bonds between the other NH and a C=O of two barbituric acid units. (b) Large scale and (c) high-resolution STM images of **2** at a liquid–solid interface between 1-phenyloctane and HOPG. In (b), domains I and II are surrounded by blue and red lines, respectively. (d) Schematic representation of proposed packing structure of **2** in **PN**.

Lengths given in these figures are based on (100) and (001) diffractions found in the powder X-ray pattern in Fig. 3.

The rearrangement of hydrogen bonded patterns from the rosette to the ester-mediated hydrogen-bonded chain could occur only through the monomeric state. In other words, **TF** is an “off-pathway” intermediate in the pathway leading to **PN**. Indeed, when the transformation kinetics was observed under an isothermal condition by monitoring the emission intensity at 650 nm ( $I_{650}$ ), the lag time became shorter upon decreasing initial monomer concentration (Fig. S9).<sup>16</sup>

In conclusion, we have demonstrated that the introduction of an ester unit into a barbiturated naphthalene supramolecular building block destabilizes gel-forming columnar stacks through the hydrogen-bonded rosettes, and could open a new pathway leading to crystalline two-dimensional nanostructures. Role of the ester group is remarkable because it not only destabilizes the interaction between rosettes but also allows the formation of new molecular sequences by intervening in hydrogen bond formation. The rosette-based supramolecular polymers covered with long alkyl chains show sufficient solubility in MCH, thus act as gel-forming nanostructures. In contrast, the ester-mediated hydrogen-bonded chains promote their two-dimensional organization because of the exposed  $\pi$ -conjugated unit, thus affording crystalline platelike nanostructures. The distinct material properties of these supramolecular polymorphic states are expected to show smart optoelectronic properties by introducing more functional  $\pi$ -conjugated units, which is on-going in our group.

This work was supported by the Japan Society for the Promotion of Science (JSPS) KAKENHI Grant Number 19H02760. S.Y. also acknowledges financial support from the The Murata Science Foundation. K. A. also acknowledges financial support from JSPS for a research fellowship for young scientists (17J02520).

### Conflicts of interest

There are no conflicts to declare.

### Notes and references

- (a) A. Das, B. Maity, D. Koley and S. Ghosh, *Chem. Commun.*, 2013, **49**, 5757–5759; (b) T. Fukui, S. Kawai, S. Fujinuma, Y. Matsushita, T. Yasuda, T. Sakurai, S. Seki, M. Takeuchi and K. Sugiyasu, *Nat. Chem.*, 2017, **9**, 493–499; (c) N. M. Matsumoto, R. P. M. Laffleur, X. Lou, K. C. Shih, S. P. W. Wijnands, C. Guibert, J. W. A. M. Van Rosendaal, I. K. Voets, A. R. A. Palmans, Y. Lin and E. W. Meijer, *J. Am. Chem. Soc.*, 2018, **140**, 13308–13316; (d) J. Matern, Y. Dorca, L. Sanchez and G. Fernandez, *Angew. Chem., Int. Ed.* 2019, **58**, 16730–16740; (e) M. Wehner, M. I. S. Röhr, M. Bühler, V. Stepanenko, W. Wagner and F. Würthner, *J. Am. Chem. Soc.*, 2019, **141**, 6092–6107.
- (a) F. J. M. Hoeben, P. Jonkhelijm, E. W. Meijer and A. P. H. J. Schenning, *Chem. Rev.*, 2005, **105**, 1491–1546; (b) S. Yagai, *Bull. Chem. Soc. Jpn.*, 2015, **88**, 28–58; (c) S. S. Babu, V. K. Praveen and A. Ajayaghosh, *Chem. Rev.*, 2014, **114**, 1973–2129.
- (a) S. Yagai, M. Usui, T. Seki, H. Murayama, Y. Kikkawa, S. Uemura, T. Karatsu, A. Kitamura, A. Asano and S. Seki, *J. Am. Chem. Soc.*, 2012, **134**, 7983–7994; (b) S. Yagai, S. Okamura, Y. Nakano, M. Yamauchi, K. Kishikawa, T. Karatsu, A. Kitamura, A. Ueno, D. Kuzuhara, H. Yamada, T. Seki and H. Ito, *Nat. Commun.*, 2014, **5**, 4013; (c) S. Yagai, T. Seki, H. Aonuma, K. Kawaguchi, T. Karatsu, T. Okura, A. Sakon, H. Uekusa and H. Ito, *Chem. Mater.*, 2016, **28**, 234–241.
- (a) J. C. MacDonald and G. M. Whitesides, *Chem. Rev.*, 1994, **94**, 2383–2420; (b) T. L. Threlfall, *Analyst*, 1995, **120**, 2435–2460; (c) T. Kato, *Science*, 2002, **295**, 2414–2418; (d) J. T. Davis and G. P. Spada, *Chem. Soc. Rev.*, 2007, **36**, 296–313; (e) M. J. Mayoral, N. Bilbao and D. González-Rodríguez, *ChemistryOpen*, 2016, **5**, 10–32.
- (a) N. Zencirci, T. Gelbrich, V. Kahlenberg and U. J. Griesser, *Cryst. Growth Des.*, 2009, **9**, 3444–3456; (b) D. Rossi, T. Gelbrich, V. Kahlenberg and U. J. Griesser, *CrystEngComm*, 2012, **14**, 2494–2506; (c) T. Gelbrich, I. Meischberger and U. J. Griesser, *Acta Crystallogr. Sect. C Struct. Chem.*, 2015, **71**, 204–210.
- S. Yagai, Y. Kitamoto, S. Datta and B. Adhikari, *Acc. Chem. Res.*, 2019, **52**, 1325–1335.
- B. Adhikari, X. Lin, M. Yamauchi, H. Ouchi, K. Aratsu and S. Yagai, *Chem. Commun.*, 2017, **53**, 9663–9683.
- (a) S. Yagai, Y. Goto, X. Lin, T. Karatsu, A. Kitamura, D. Kuzuhara, H. Yamada, Y. Kikkawa, A. Saeki and S. Seki, *Angew. Chem., Int. Ed.*, 2012, **51**, 6643–6647; (b) M. Yamauchi, B. Adhikari, D. D. Prabhu, X. Lin, T. Karatsu, T. Ohba, N. Shimizu, H. Takagi, R. Haruki, S. I. Adachi, T. Kajitani, T. Fukushima and S. Yagai, *Chem. - Eur. J.*, 2017, **23**, 5270–5280.
- (a) S. Yagai, Y. Goto, T. Karatsu, A. Kitamura and Y. Kikkawa, *Chem. - Eur. J.*, 2011, **17**, 13657–13660; (b) B. Adhikari, K. Aratsu, J. Davis and S. Yagai, *Angew. Chem., Int. Ed.*, 2019, **58**, 3764–3768; (c) K. Aratsu, N. Shimizu, H. Takagi, R. Haruki, S. Adachi and S. Yagai, *Chem. Lett.*, 2020, **49**, 178–181.
- (a) B. Adhikari, Y. Yamada, M. Yamauchi, K. Wakita, X. Lin, K. Aratsu, T. Ohba, T. Karatsu, M. J. Hollamby, N. Shimizu, H. Takagi, R. Haruki, S. I. Adachi and S. Yagai, *Nat. Commun.*, 2017, **8**, 15254; (b) D. D. Prabhu, K. Aratsu, Y. Kitamoto, H. Ouchi, T. Ohba, M. J. Hollamby, N. Shimizu, H. Takagi, R. Haruki, S. Adachi, S. Yagai, *Sci. Adv.*, 2018, **4**, eaat8466; (c) K. Aratsu and S. Yagai et al., *Nat. Commun. in press*.
- Y. Kitamoto, Z. Pan, D. D. Prabhu, A. Isobe, T. Ohba, N. Shimizu, H. Takagi, R. Haruki, S. Adachi and S. Yagai, *Nat. Commun.*, 2019, **10**, 4578.
- B. M. Rosen, C. J. Wilson, D. A. Wilson, M. Peterca, M. R. Imam and V. Percec, *Chem. Rev.*, 2009, **109**, 6275–6540.
- A. Suzuki, K. Aratsu, S. Datta, N. Shimizu, H. Takagi, R. Haruki, S. Adachi, M. Hollamby, F. Silly and S. Yagai, *J. Am. Chem. Soc.*, 2019, **141**, 13196–13202.
- (a) T. F. A. De Greef, M. M. J. Smulders, M. Wolffs, A. P. H. J. Schenning, R. P. Sijbesma and E. W. Meijer, *Chem. Rev.*, 2009, **109**, 5687–5754; (b) M. M. J. Smulders, M. M. L. Nieuwenhuizen, T. F. A. de Greef, P. van der Schoot, A. P. H. J. Schenning and E. W. Meijer, *Chem. - Eur. J.*, 2010, **16**, 362–367.
- (a) X. Feng, W. Pisula, L. Zhi, M. Takase and K. Müllen, *Angew. Chem., Int. Ed.*, 2008, **47**, 1703–1706; (b) T. Osawa, T. Kajitani, D. Hashizume, H. Ohsumi, S. Sasaki, M. Takata, Y. Koizumi, A. Saeki, S. Seki, T. Fukushima and T. Aida, *Angew. Chem., Int. Ed.*, 2012, **51**, 7990–7993; (c) C. Kulkarni, K. K. Bejagam, S. P. Senanayak, K. S. Narayan, S. Balasubramanian and S. J. George, *J. Am. Chem. Soc.*, 2015, **137**, 3924–3932.
- P. A. Korevaar, S. J. George, A. J. Markvoort, M. M. J. Smulders, P. A. J. Hilbers, A. P. H. J. Schenning, T. F. A. De Greef and E. W. Meijer, *Nature*, 2012, **481**, 492–496.